

A DUAL-BAND BANDPASS FILTER WITH A TUNABLE PASSBAND

Dinghong Jia, Quanyuan Feng*, Xiaoguo Huang, and Qianyin Xiang

School of Information Science and Technology, Southwest Jiaotong University, Chengdu, Sichuan 610031, China

Abstract—In this paper, a novel dual-band bandpass filter with a tunable passband is proposed. Based on two quarter-wavelength resonators and one half-wavelength resonator, dual-band character is designed by introducing two independent coupling paths. The filter structure is designed and can be divided into two parts. The Transmission Zeros (TZs) are derived through simulation. By varying the reverse bias voltage applied to the varactor diodes which are connected to the resonators, the first passband can be independently tuned. The second passband can be easily controlled by the width of the half-resonator. Finally, simulation results show a first tunable passband with a constant fractional-bandwidth of $3.9 \pm 0.3\%$, a center frequency of 1.472–1.886 GHz, and the second passband almost remains constant with a fractional-bandwidth 2.4% at frequency range 2.24 GHz. The measurement of the fabricated example shows good agreement with the simulation.

1. INTRODUCTION

In recent years, as an indispensable part of RF front ends, filters have gained a lot of attention due to the rapid development of modern communication systems, e.g., wireless local area networks (WLAN), global system for mobile communications (GSM), the third generation (3G), the fourth generation (4G), worldwide interoperability for microwave access (WiMax), etc. Due to the demands on working in multiband, the multiband bandpass filters, especially dual-band filters [1–4], become a hot research issue.

Due to their potential to significantly reduce the overall size and complexity of modern multiband communication systems, RF tunable

Received 12 December 2012, Accepted 21 January 2013, Scheduled 1 February 2013

* Corresponding author: Quanyuan Feng (fengquanyuan@163.com).

filters are becoming an active research topic [5–15]. However, none of the above tunable filters have addressed the issue on designing two tunable passbands. There are several works [16–20] on tunable dual-band bandpass filters. Among them, [16–18] focused on the design of fixed first passband and tunable second passband. No attention has been paid to independent dual-band tuning. [19] demonstrated a varactor-tuned dual-band tunable BPF that both passbands can be independently tuned at the cost of a large circuit size, large number of varactor diodes, large insertion loss. In [20], the authors presented a tunable dual-band BPF based on two varactor-tuned resonators. The proposed filter structure offers a possibility of two tunable passbands with a fixed first passband and a controllable second passband or both passbands tuned together. Yet its two passbands could not be tuned independently with any influence on the other passband.

In this paper, a dual-band BPF with a tunable first passband and easily controlled second passband characteristics is presented. Each passband can be independently controlled and has a tiny influence on the other. The dual-band character is profited from the two independent coupling schemes that do not disturb with each other. The first passband is generated by the input/output couplings and two varactor-loaded open-loop resonators; meanwhile, the second passband is determined by the input/output couplings and the half-wavelength resonator. The filter can be completely divided into two independent filters and analyzed. The design procedure for the element parameters is given. The measured performance of the fabricated filter shows good agreement with the proposed theory.

2. FILTER DESIGN

Figure 1 shows the layout of the proposed reconfigurable dual-band bandpass filter. The dual-band bandpass filter consists of two $1/4$ wavelength varactor-loaded open-loop resonators, one $1/2$ wavelength resonator and the coupling input/output. Two chip capacitors C_g are adopted to optimize the return loss and insertion loss to achieve a better performance in the tuning range. As the two quarter resonators and the half-wavelength resonator are only coupled with the in/out ports, the filter structure can be divided into two independent filters with the original parameters, as shown in Figures 2(b) and (c). The simulation results are presented in Figure 2(a). Hence, the mechanism producing each passband and transmission zeros is readily discovered. It is observed that the dual-band characteristics can be achieved by combining two independent bandpass filter together, and TZ1 and TZ2 are generated by Filer I and cross couplings, respectively.

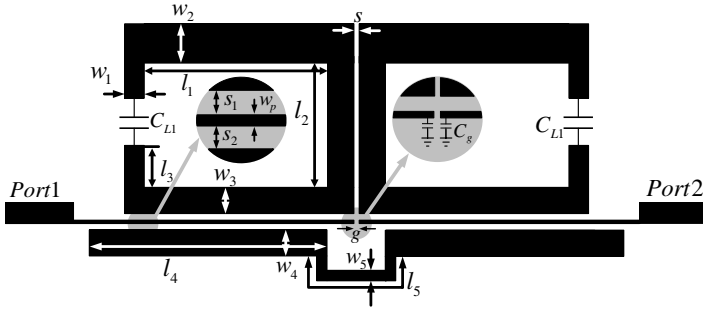


Figure 1. Layout of the proposed reconfigurable dual-band bandpass filter.

For the two order BPF as shown in Figure 2(a), the input admittance seen from port 3 and port 4 can be defined as

$$Y_{in,o,e} = \Delta Y_{o,e} / Y_{22o,e} \quad (1)$$

$$Y_{o,e} = \begin{bmatrix} D_{o,e}/B_{o,e} + j\omega C_L & -\Delta A/B_{o,e} - j\omega C_L \\ -1/B_{o,e} - j\omega C_L & -A_{o,e}/B_{o,e} + j\omega C_L \end{bmatrix} \quad (2)$$

$$\Delta A = A_{o,e}D_{o,e} - B_{o,e}C_{o,e} \quad (3)$$

$$A = A_1 \cdot A_{2o,2e} \cdot A_{3o,3e} \cdot A_4 \quad (4)$$

$$A_{1,4} = \begin{bmatrix} \cos \phi_{1,4} & j \sin \phi_{1,4} / Y_{1,4} \\ j \sin \phi_{1,4} Y_{1,4} & \cos \phi_{1,4} \end{bmatrix} \quad (5)$$

$$A_{2o,e} = \begin{bmatrix} \cos \phi_{2o,e} & j \sin \phi_{2o,e} / Y_{2o,e} \\ j \sin \phi_{2o,e} Y_{2o,e} & \cos \phi_{2o,e} \end{bmatrix} \quad (6)$$

$$A_{3o,e} = \begin{bmatrix} X_{11} & X_{12} \\ X_{21} & X_{22} \end{bmatrix} \quad (7)$$

where

$$X_{11} = \frac{2(\cos \phi_{3o} \cos \phi_{3e} + 1) - \sin \phi_{3o} \sin \phi_{3e} (Y_{3o}/Y_{3e} + Y_{3e}/Y_{3o})}{2(\cos \phi_{3o} + \cos \phi_{3e})},$$

$$X_{12} = j \frac{\sin \phi_{3o} \cos \phi_{3e} / Y_{3o} + \cos \phi_{3o} \sin \phi_{3e} / Y_{3e}}{\cos \phi_{3o} + \cos \phi_{3e}},$$

$$X_{21} = j \frac{\sin \phi_{3o} \cos \phi_{3e} Y_{3o} + \cos \phi_{3o} \sin \phi_{3e} Y_{3e}}{\cos \phi_{3o} + \cos \phi_{3e}},$$

$$X_{22} = \frac{2 \cos \phi_{3o} \cos \phi_{3e}}{\cos \phi_{3o} + \cos \phi_{3e}}.$$

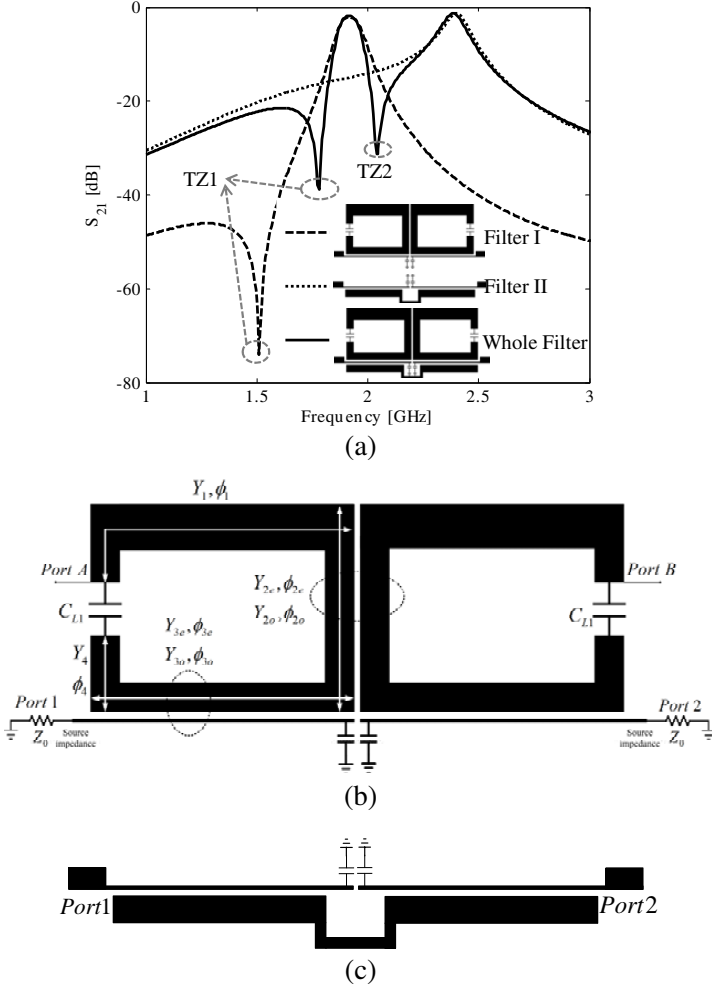


Figure 2. (a) Simulations of S_{21} of Filter I, Filter II, and whole structure. (b) Layout of Filter I. (c) Layout of Filter II.

The overall admittance matrix of capacitively loaded coupled resonator is

$$[Y] = \begin{bmatrix} \frac{Y_{in-e} + Y_{in-o}}{2} & \frac{Y_{in-e} - Y_{in-o}}{2} \\ \frac{Y_{in-e}}{2} - \frac{Y_{in-o}}{2} & \frac{Y_{in-e}}{2} + \frac{Y_{in-o}}{2} \end{bmatrix} \quad (8)$$

For the above overall admittance matrix, three conditions must be satisfied. One is the resonance condition, and the others are the

coupling condition, Q_{ext} . Conditions are

$$\text{Im}(Y_{11}(\omega_0))=0 \quad \frac{\text{Im}(Y_{12}(\omega_0))}{b} = K_{12} \quad Q_{ext} = \frac{b}{\text{Re}[Y_{11}(\omega_0)]} = \frac{g_0 g_1}{\Delta} \quad (9)$$

where

$$b = \frac{\omega_0}{2} \frac{\partial \text{Im}(Y_{11}(\omega_0))}{\partial \omega} \quad K_{12} = \frac{\Delta}{\sqrt{g_1 g_2}} \quad (10)$$

For simplicity and convenience to confirm the design parameters $Y_1, Y_{2e,o}, Y_{3e,o}, Y_4, w_1, w_2, w_3, l_1, l_2, l_3$, the loading capacitor C_{L1} can be decoupled from $\text{Im}(Y_{11}(\omega_0)) = 0$ (9), then C_{L1} can be rewritten as

$$C_{L1} = \frac{1}{j\omega} \text{Im} \left[\frac{C_o + C_e}{A_o + A_e + B_o D_o + B_e D_e - \Delta A_o - \Delta A_e - 2} \right] \Big|_{\omega=\omega_0} \quad (11)$$

With C_{L1} and the above equations, the other design parameters can be determined.

The one order filter determines the second passband, as shown in Figure 2(c). Its center frequency is mainly controlled by the length ($2l_4 + l_5$) of the half-wavelength resonator, as shown by formula (12). Q_{ext} determines the bandwidth of the passband. The method to extract the Q_{ext} is shown in [21].

$$f_c = \frac{c}{2(2l_4 + l_5)\sqrt{\varepsilon_e}} \quad (12)$$

By employing the aforementioned method, the tunability of Filters I and II is shown in Figure 3. The load capacitors C_{L1} are implemented with lump chip capacitors ($1.5 \times 0.7 \text{ mm}^2$), where SMV 1405 abrupt junction tuning varactors of SKYWORKS in SC-79 package have been used as the tuning elements. The single capacitances are 0.63 pF and 2.67 pF at 30 V and 0 V bias, respectively. The Spice Model of the SMV1405 is adopted in the simulation.

Then we can assembled Filters I and II together. The external quality factors, Q_{e1} and Q_{e2} , of the two bands can be extracted [21], respectively. As shown in Figures 4(a), when the coupled gap width s_1 varies from 0.1 mm to 0.4 mm, Q_{e1} increases from 28.9 to 122. Simultaneously, Q_{e2} hardly changes and basically stays the same. When s_2 changes from 0.1 mm to 0.4 mm, Q_{e2} increases from 11.2 to 17.6, and Q_{e1} remains in a narrow band 28.9 to 25.0. Additionally, a detailed analysis of the coupling gap g between the input and output ports is presented in Figure 4(c). The gap has a small effect on the insertion loss and the coupling. By observing Figure 4, the design guidelines of the feed circuit can be provided, and the initial feed part of the proposed filter can be determined independently.

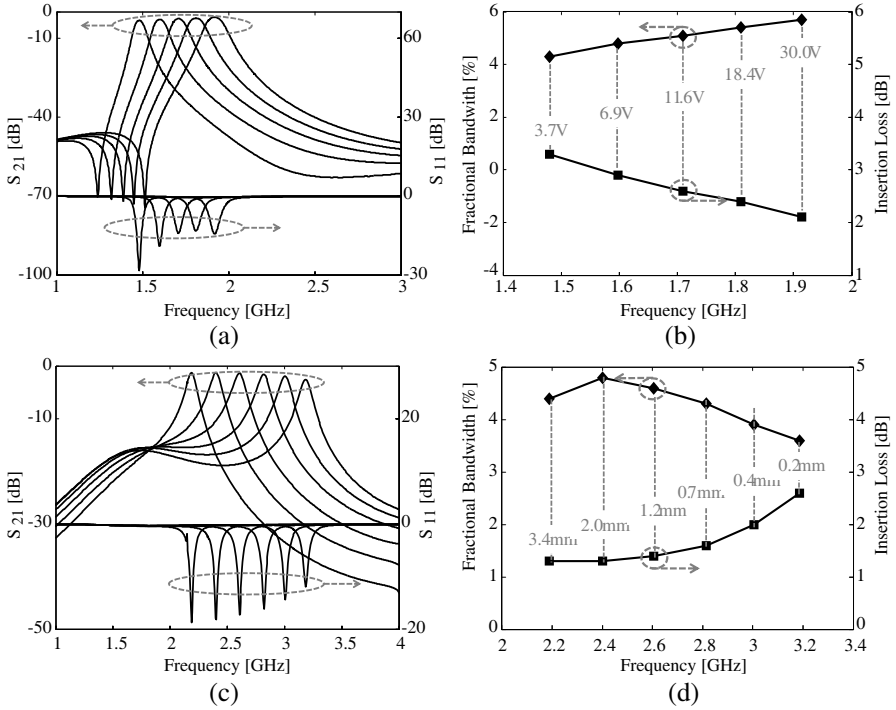


Figure 3. (a) Tunability of Filter I. (b) Simulated insertion loss and 3-dB fractional bandwidth of Filter I under the bias voltage v_1 ($s_1 = 0.1$ mm). (c) Tunability of Filter II. (d) Simulated insertion loss and 3-dB absolute bandwidth of Filter II under the width w_4 ($s_2 = 0.1$ mm).

From the analysis above, we can achieve a configurable BPF Filter with a predefined constant fractional-bandwidth first passband and a controllable second passband with constant absolute bandwidth. The simulation results are shown in Figure 5. Obviously, the first passband shows a tuning range 1.449–1.889 GHz, a insertion loss of 3.642–1.967 dB, a constant fractional bandwidth of $4.35 \pm 0.55\%$, and the second passband remains constant during the tuning process. The second passband can be controlled in the frequency range of 2.26–3.26 GHz with an absolute bandwidth of 105 ± 11 MHz, an insertion loss of 2.265–3.165 dB. Meanwhile, the first passband can hardly be influenced, as shown in Figure 5(b).

The design procedure of the presented configurable dual-band BPF is given as follows: Firstly, determine the dimensions of Filters

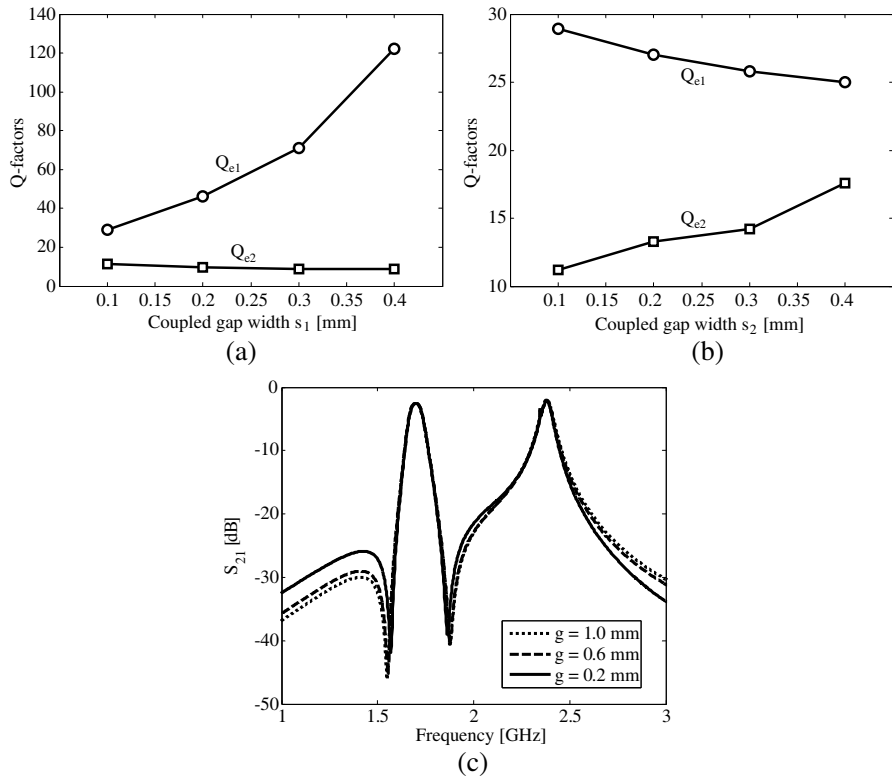


Figure 4. (a) The Q -factors as function of s_1 ($s_2 = 0.1$ mm). (b) The Q -factors as function of s_2 ($s_1 = 0.1$ mm). (c) The S_{21} as function of g ($s_1 = 0.1$ mm, $s_2 = 0.2$ mm).

I and II to achieve tuning ranges and bandwidths. Next, determine feed line dimensions according to Figure 4. Finally, the optimized dual-band configurable BPF can be achieved.

3. FABRICATION AND MEASUREMENTS

To demonstrate the performance of the proposed filter, a tunable filter is designed and fabricated, as shown in Figure 6. The dimensions for the filter are presented in Table 1 for $\epsilon_r = 2.65$, $h = 0.5$ mm with $w_4 = 2$ mm, $s_1 = 0.1$ mm, $s_2 = 0.2$ mm. The dc bias is done by using a 100 k Ω resistor and an ATC chip capacitor between the DC voltage and the open ends of the resonator. v_1 is the bias voltage of C_{L1} . The capacitor-varactor series connection hardly changes the overall

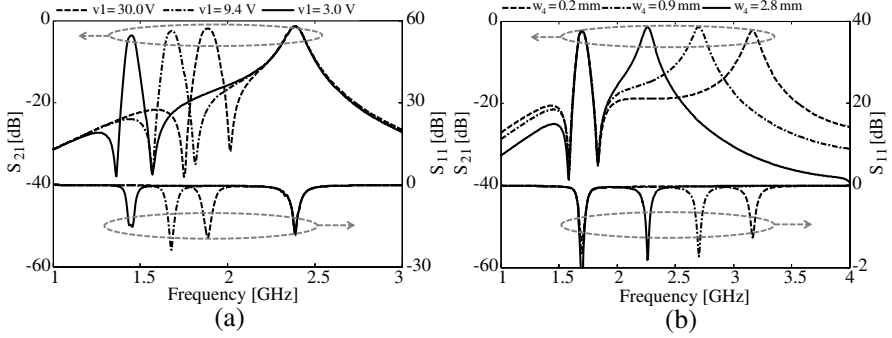


Figure 5. (a) The tuning range of first passband under different bias voltage ($s_1 = 0.1$ mm, $s_2 = 0.1$ mm). (b) The tuning range of second passband under different width w_4 ($s_1 = 0.1$ mm, $s_2 = 0.1$ mm).

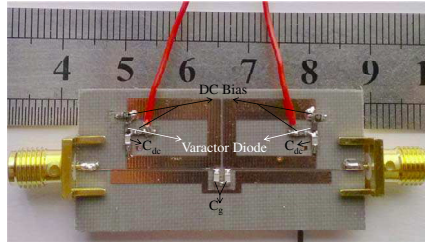


Figure 6. Fabricated configurable dual-band BPF.

Table 1. Critical dimensions of the bandwidth tunable BPF with harmonic suppression (Unit: mm).

l_1	l_2	l_3	l_4	l_5	w_1	w_2	w_3	w_5	w_p	s	g
11.8	5.6	2.2	15.1	9.0	0.8	3.3	2.0	0.6	0.3	0.2	0.2

capacitance with the chip capacitor value 15 pF. The C_g is selected as 0.6 pF as a tradeoff between tunability and loss.

The simulated and measured results are presented in Figure 7. Clearly, the first passband shows a constant fractional-bandwidth range of $3.9 \pm 0.3\%$, a center frequency of 1.472–1.886 GHz, a insertion loss of 4.2–5.7 dB while the bias voltage v_1 changes from 30.0 to 3.0 V. Among the first passband tuning process, the second passband exhibits a small variation with center frequency of 2.24 GHz, an absolute bandwidth of 53 MHz, an insertion loss of 3.517 dB. Simulation and measurement show good agreement. The distinction

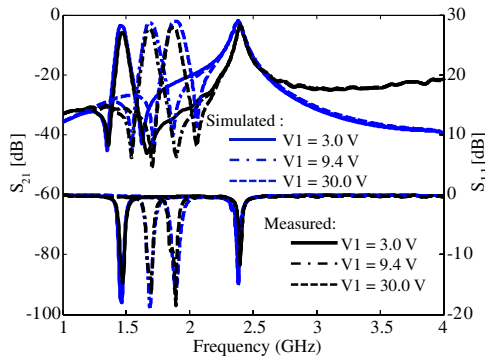


Figure 7. Simulation and measurement of fabricated configurable dual-band BPF.

Table 2. Comparison this work with others.

References	Tunability		Harmonic Suppression
	1st passband	2nd passband	
[12]	Fixed @ 2.43	5.28–5.74	NA
[13]	Fixed @ 1.15	2.12–2.51	NA
[14]	Fixed @ 1.58	2.38–2.56	NA
[15]	2.20–2.7	3.45–4.20	–20 dB to $1.75f_2$
[16]	0.85–1.20	1.40–2.14	–20 dB to $10f_2$
This work	1.45–1.89	Fixed @ 2.24 (easily controlled during 2.26–3.26)	–16 dB to $1.8f_2$

between simulation and measurement is mainly due to the mismatching tolerance.

Table 2 compares the proposed filter with some recent state-of-the-art designs. It is summarized that our presented filter shows the widest dual-band easily controlled range.

4. CONCLUSION

In this paper, a dual-band bandpass filter with two independent configurable passbands is demonstrated. By introducing two independent coupling paths, the proposed filter shows a unique property that each passband can hardly be influenced while tuning the other passband. This design method is verified by simulated and

measured results and shows good performance. In the future, the use of RF MEMS will significantly enhance the performance of filters, and DGS can be introduced to suppress the harmonic.

ACKNOWLEDGMENT

This work is supported by the National Natural Science Foundation of China (NNSF) under Grant 60990320, 60990323, 61271090, the National 863 Project of China under Grant 2012AA012305, Sichuan Provincial Science and technology support Project under Grant 2012GZ0101, and Chengdu Science and technology support Project under Grant 12DXYB347JH-002.

REFERENCES

1. Guan, X.-H., W. Fu, G.-H. Li, S. Jiang, and H.-W. Liu, "Novel microstrip dual-band bandpass filter with wide stopband and high isolation," *Microwave and Optical Technology Letters*, Vol. 53, 803–806, 2011.
2. Tang, C.-W. and P.-H. Wu, "Design of a planar dual-band bandpass filter," *IEEE Microwave Wireless Component Letter*, Vol. 21, 362–364, 2011.
3. Gao, L. and X.-Y. Zhang, "Novel dual-band bandpass filters using sub-loaded short-ended resonators," *Microwave and Optical Technology Letters*, Vol. 54, 2771–2774, 2012.
4. Zhang, X.-S., B. Liu, Y.-J. Zhao, J.-K. Wang, and W. Chen, "Compact and high selectivity dual-band dual-mode microstrip BPF with five transmission zeros," *Microwave and Optical Technology Letters*, Vol. 54, 79–81, 2012.
5. Park, S.-J. and G. M. Rebeiz, "Low-loss two-pole tunable filters with three different predefined bandwidth characteristics," *IEEE Transactions on Microwave Theory and Techniques*, Vol. 56, 1137–1148, 2008.
6. Wang, X. G., X. H. Cho, and S. W. Yun, "A tunable combline bandpass filter loaded with series resonator," *IEEE Transactions on Microwave Theory and Techniques*, Vol. 60, 1569–1576, 2012.
7. Lacorte Caniato Serrano, A., F. Saletto Herrera, T. P. Vuong, and P. Ferrari, "Synthesis methodology applied to a tunable patch filter with independent frequency and bandwidth control," *IEEE Transactions on Microwave Theory and Techniques*, Vol. 60, 484–493, 2012.

8. Wang, Y. Y., F. Wang, and B. Liu, "A tunable bandpass filter with constant bandwidth based on one ring resonator," *Journal of Electromagnetic Waves and Applications*, Vol. 26, Nos. 11–12, 1587–1593, 2012.
9. Liu, B., F. Wei, H. Zhang, and X. Shi, "A tunable bandpass filter with switchable bandwidth," *Journal of Electromagnetic Waves and Applications*, Vol. 25, Nos. 2–3, 223–232, 2011.
10. Park, W. Y. and S. Lim, "Bandwidth tunable and compact band-pass filter (BPF) using complementary split ring resonators (CSRRS) on substrate integrated waveguide (SIW)," *Journal of Electromagnetic Waves and Applications*, Vol. 24, Nos. 17–18, 2407–2417, 2010.
11. Xiang, Q. Y., Q. Y. Feng, and X. G. Huang, "Half-mode substrate integrated waveguide (HMSIW) filters and its application to tunable filters," *Journal of Electromagnetic Waves and Applications*, Vol. 25, Nos. 14–15, 2043–2053, 2011.
12. Li, L. and D. Uttamchandani, "Demonstration of a tunable RF MEMS bandpass filter using silicon foundry process," *Journal of Electromagnetic Waves and Applications*, Vol. 23, Nos. 2–3, 405–413, 2009.
13. Zhang, X. Y., Y. B. Zhang, X. Y. Wang, and B.-J. Hu, "Tunable bandpass filter with continuously-tuned center frequency and bandwidth," *Journal of Electromagnetic Waves and Applications*, Vol. 26, Nos. 8–9, 1048–1058, 2012.
14. Wei, F., L. Chen, X. W. Shi, and C.-J. Gao, "UWB bandpass filter with one tunable notch-band based on DGS," *Journal of Electromagnetic Waves and Applications*, Vol. 26, Nos. 5–6, 673–680, 2012.
15. Jahromi, M. N., "Novel compact meta-material tunable quasi elliptic band-pass filter using microstrip to slotline transition," *Journal of Electromagnetic Waves and Applications*, Vol. 24, Nos. 17–18, 2371–2382, 2010.
16. David, G., L. Antonio, M. Esther, M. Diego, and L. Pradell, "Tunable dual-band bandpass filter for WLAN applications," *Microwave and Optical Technology Letters*, Vol. 51, 2025–2028, 2009.
17. Zhang, X. Y. and Q. Xue, "Novel centrally loaded resonators and their applications to bandpass filters," *IEEE Transactions on Microwave Theory and Techniques*, Vol. 56, 913–921, 2008.
18. Chaudhary, G., H. Choi, Y. Jeong, J. Kim, D. Kim, and J. C. Kim, "Design of dual-band bandpass filter using DGS with controllable second passband," *IEEE Microwave and Wireless Components*

- Letters*, Vol. 21, 589–591, 2011.
19. Djoumessi, E. E., M. Chaker, and K. Wu, “Varactor-tuned quarter-wavelength dual-bandpass filter,” *IET Microwave, Antennas & Propagation*, Vol. 3, 117–124, 2009.
 20. Chaudhary, G., Y. Jeong, and J. Kim, “Harmonic suppressed dual-band bandpass filters with tunable passbands,” *IEEE Transactions on Microwave Theory and Techniques*, Vol. 60, 2115–2123, 2012.
 21. Hong, J. S. and M. J. Lancaster, *Microstrip Filters for RF/Microwave Applications*, Wiley, New York, 2001.